

Growth dominates choice in network percolation

Vikram S. Vijayaraghavan,^{1,2} Pierre-André Noël,^{2,3} Alex Waagen,^{2,4} and Raissa M. D'Souza^{2,3,5,6}

¹*Department of Physics, University of California, Davis, California 95616, USA*

²*Complexity Sciences Center, University of California, Davis, California 95616, USA*

³*Department of Computer Science, University of California, Davis, California 95616, USA*

⁴*Department of Mathematics, University of California, Davis, California 95616, USA*

⁵*Department of Mechanical and Aerospace Engineering, University of California, Davis, California 95616, USA*

⁶*The Santa Fe Institute, Santa Fe, New Mexico 87501, USA*

(Received 12 July 2013; revised manuscript received 3 September 2013; published 30 September 2013)

The onset of large-scale connectivity in a network (i.e., percolation) often has a major impact on the function of the system. Traditionally, graph percolation is analyzed by adding edges to a fixed set of initially isolated nodes. Several years ago, it was shown that adding nodes as well as edges to the graph can yield an infinite order transition, which is much smoother than the traditional second-order transition. More recently, it was shown that adding edges via a competitive process to a fixed set of initially isolated nodes can lead to a delayed, extremely abrupt percolation transition with a significant jump in large but finite systems. Here we analyze a process that combines both node arrival and edge competition. If started from a small collection of seed nodes, we show that the impact of node arrival dominates: although we can significantly delay percolation, the transition is of infinite order. Thus, node arrival can mitigate the trade-off between delay and abruptness that is characteristic of explosive percolation transitions. This realization may inspire new design rules where network growth can temper the effects of delay, creating opportunities for network intervention and control.

DOI: [10.1103/PhysRevE.88.032141](https://doi.org/10.1103/PhysRevE.88.032141)

PACS number(s): 64.60.ah, 64.60.aq, 89.75.Hc, 02.50.Ey

I. INTRODUCTION

Real-world networks are not static but instead have structures that evolve in time [1–5]. This dynamical aspect can have implications for important network properties such as the extent of connectivity among nodes, nodal degree distributions, and degree-degree correlations [6–11]. The onset of large-scale connectivity is typically modeled as a percolation phase transition [12–14]. Despite the dynamic nature of a network, most models of percolation analyze the connectivity among a fixed collection of N initially isolated nodes, similar to the seminal Erdős-Rényi model [15]. Edges chosen uniformly at random from all possible edges are then added to the graph. From a different perspective, node arrival is also a natural consideration, as captured by seminal network growth models such as preferential attachment [6], growth by copying [16], and duplication-mutation mechanisms [17].

Several years ago, a variant of the Erdős-Rényi percolation model that includes node arrival was introduced by Callaway *et al.* [7]. The model, which we call the CHKNS model after the initials of the authors, showed that the percolation transition is much smoother with node arrival, where the number of nodes increases as the expected edge density remains fixed [7,18]. In this case, we have a *randomly grown graph* as opposed to a random graph. The process starts from a collection of one or two isolated nodes. At each discrete time step, a node is added to the graph and then with probability δ an edge is added between two nodes chosen uniformly at random. All nodes connected together by following a path of edges form a *component*, and as δ increases, so too does the expected size of components. The percolation transition corresponds to the emergence of a “giant component” (i.e., a component that contains a finite fraction of all the nodes), and the critical value for this transition in the CHKNS model was shown to be $\delta_c = 1/8$ [7].

Rather than the second-order phase transition that characterizes typical percolation transitions [12–14], the CHKNS transition is much smoother (it is of infinite order) [19]. Furthermore, when a node is picked at random, the average size of the component to which that node belongs (traditionally referred to as the susceptibility) exhibits a discrete jump at the critical point but remains finite. Introducing the idea that growth in a system can lead to a very different behavior and showing that these effects stem from high degree-degree correlations between nodes that arrive early during the process are two significant contributions made by the CHKNS model.

More recently, the notion of competition among arriving edges was shown to alter the location and nature of the percolation phase transition [20]. Starting from a collection of N isolated nodes, at each time step a set of m candidate edges are chosen uniformly at random, where m is a fixed constant. The consequences of adding each edge is examined and only the single edge that minimizes or maximizes a predefined criteria is actually added to the graph; the other candidate edges are discarded. Criteria that delay the onset of percolation can also alter the nature of the transition, leading to an extremely abrupt change in large scale connectivity that appears discontinuous for any finite system [21–24]. Such abrupt transitions are referred to as “explosive percolation.”

In this paper, we combine the two approaches: node arrival, which is known to lead to a smoother transition, and competition between edges, which is known to lead to an abrupt “explosive” transition. The process analyzed begins with two isolated nodes. At each discrete time step a new node arrives and, with probability δ , we add an edge to the graph via a competitive process called the “adjacent edge” (AE) rule [25] (defined explicitly in Sec. II). We call this model the AE-CHKNS model, as it combines the AE rule with the CHKNS model. As expected, we find that the critical

point of the AE-CHKNS model is significantly delayed when compared to that for the original CHKNS model. Surprisingly, we find that the AE-CHKNS model results in a smooth, infinite-order phase transition with scaling behavior similar to the CHKNS model. However, the average size of a component when a node is picked at random (the susceptibility) diverges at the critical point, whereas in the original CHKNS model susceptibility remains finite with a discrete jump at the critical point.

Hence, edge competition in a graph with node arrival is fundamentally different from edge competition in a system where the number of nodes is static. In the latter, competition leads to an extremely abrupt percolation transition [20,22,23,25] and in the former the transition can be infinitely smooth. This suggests that introducing node arrival into models of percolation with edge competition provides opportunities to effectively delay the onset of large-scale connectivity, but without the accompanying abruptness of “explosive percolation” transitions. This may be a desirable feature in many circumstances. For instance, in an abrupt transition, the instant the system transitions to the supercritical regime, a large fraction of the network is already connected together. In contrast, in an infinitely smooth transition, only a small fraction of the nodes are in the largest component as we enter the supercritical regime, allowing ample time for detection of large-scale connectivity and for network interventions.

II. MODELS OF NETWORK GROWTH

Here we combine two prominent ideas in the study of complex networks: growth and choice. In Secs. II A and II B, we explicitly define the existing models, which form the basis for the hybrid model that we then introduce in Sec. II C. In Sec. III, we analyze the hybrid model focusing on the emergence of a giant component as we increase the control parameter δ . The parameter δ denotes the expected edge density, becoming exact in the limit of number nodes going to infinity.

A. CHKNS process

CHKNS is a model of network growth with node and edge arrival. Starting from a small collection of seed nodes, at each time step a node is added, and with probability δ a random edge is added between any two existing nodes chosen uniformly at random. Formally, the CHKNS model is defined as follows. Starting with one isolated node at time $t = 1$, at each discrete time step:

- (1) A node is added to the graph.
- (2) With probability δ , an edge is added to the graph between two nodes chosen uniformly at random from the set of all nodes, including the node just added.
- (3) If $t < N$, set $t \rightarrow t + 1$ and return to step 1. Stop when $t = N$.

In the limit $N \rightarrow \infty$, the model has an infinite-order phase transition at $\delta = 1/8$ [7]. We note that the critical value of δ is much smaller when compared to standard Erdős-Rényi percolation, which has $\delta_c = 1/2$ [15]. Moreover, the nature of the resulting phase transition is extremely smooth when compared to the phase transition in the Erdős-Rényi model.

In Ref. [7] it was established that the primary reason for the difference in behaviors is due to the high degree-degree correlations that arise due to the time-ordered arrival of nodes. The simplicity and tractable nature of the model has inspired rigorous analysis [18,19] and the model has been applied in a variety of different settings such as modeling email networks and the spread of computer viruses [26], modeling the spread of epidemics [27], and analyzing social networks [28] and protein interaction networks [29,30].

B. AE percolation

The adjacent edge (AE) percolation model starts from a collection of N -isolated nodes, and edges are then added in a competitive manner. First, a node is chosen uniformly at random. Then two other nodes are chosen, again uniformly at random, and the edge connecting the first node to the second node and the edge connecting the first node to the third node are examined (i.e., both potential edges are *adjacent*, sharing the first vertex in common). The edge that leads to a smaller component is added and the other is discarded. (If both candidate edges would result in the same size component, one of them is chosen at random and added to the graph.) Thus, starting with N -isolated nodes at time $t = 0$, the process can be stated formally as follows [31]. At each discrete time step:

- (1) With probability δ , an edge is added to the graph according to the rule defined above.
- (2) If $t < N$, set $t \rightarrow t + 1$ and return to step 1. We stop when $t = N$.

In the limit of $N \rightarrow \infty$, the phase transition occurs at approximately $\delta \approx 0.796$ [25]. This value is larger than for the Erdős-Rényi model (which has $\delta_c = 1/2$), showing that the addition of choice delays the phase transition. Although the phase transition looks discontinuous for finite-system sizes [25], it has been shown via analytic arguments [21–24,32,33] and rigorously proven [34] that the transition is continuous in the thermodynamic limit. Yet, the phase transition belongs to a universality class that is different from that of standard second-order phase transitions [22,33].

The AE model is a “local” process, in that with each link addition a node is first selected and that node then needs to make a choice between two options made available to it. Each step of the AE model involves three nodes (the initial node and the nodes at the end of each candidate edge) and thus involves at most three distinct components, enabling a probabilistic analysis of the evolution of component sizes [25].

C. AE-CHKNS process

Here we formally define a model combining both the CHKNS and the AE percolation processes. Starting with two isolated nodes at $t = 2$, the AE-CHKNS model is defined as follows. (See Fig. 1 for an illustration.) At each discrete time step:

- (1) A node is added to the graph.
- (2) With probability δ , an edge is added to the graph according to the AE rule.
- (3) If $t < N$, set $t \rightarrow t + 1$ and return to step 1.

We study the behavior of this system as the probability of adding an edge, δ , is varied from 0 to 1. At any time t , the total

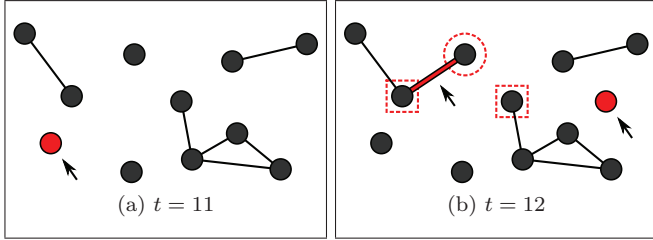


FIG. 1. (Color online) Example of the AE-CHKNS process. (a) At time $t = 11$ when a node (indicated by an arrow) is added to the graph but no edge is added. (b) The next time step, i.e., $t = 12$, when both a node and an edge (indicated by arrows) are added. To add the edge, three nodes are chosen uniformly at random. The first node (indicated with the dashed circle) must form an edge with one of two other nodes (indicated by the dashed squares), always choosing to connect to the node in the smaller component. Thus, for this example, the edge indicated by the arrow is added.

number of nodes present in the network is equal to t and the expected number of edges is δt . (Hence, edge density is δ .) We are interested in the properties of the system in the asymptotic limit $N \rightarrow \infty$. We analyze the process via both mean-field evolution equations and by Monte Carlo simulations of the direct graph evolution process. While our mean-field evolution equations are in the limit of $N \rightarrow \infty$, simulations of the growth process are always stopped at a finite N .

III. ANALYSIS

We begin by analyzing the average number of components of size k at time t , $N_k(t)$. $N_k(t)$ can be used to calculate susceptibility and the size of the largest component, two properties that are commonly used to determine the critical point at which the percolation transition occurs [14]. Our analysis is based on differential equations used to model percolation as a cluster aggregation process. See Refs. [35,36] for a general overview of such analyses, Ref. [37] for such a model that yields a discontinuous percolation transition, and Ref. [25] for a model of cluster aggregation with a choice between two edges. These are mean-field equations describing the ensemble of networks obtained from the graph evolution process.

Note that the probability of selecting a node uniformly at random from a component of size k is $kN_k(t)/t$. Then, using the notation of Ref. [25], we can define s_k , the probability that a randomly chosen node comes from a component of size k or greater:

$$s_k(t) = 1 - \sum_{j=1}^{k-1} jN_j(t)/t. \quad (1)$$

This quantity is related to the AE rule by the following argument [25]. When two nodes are picked at random, s_k^2 is the probability that both nodes come from a component of size k or greater. Thus, the probability that both nodes come from a component size $k + 1$ or greater is s_{k+1}^2 . Consider the quantity $s_k^2 - s_{k+1}^2$. It is the difference between probability of both nodes coming from components of size k or greater and the probability of both of them coming from size $k + 1$ or greater, i.e., one of the nodes should come from a component of size k and the other from a component of size k or greater. Therefore,

when two nodes are picked at random, the probability that one of them comes from a component of size k and that the other from a component of size k or greater is given by $s_k^2 - s_{k+1}^2 = 2[kN_k(t)/t]s_k - [kN_k(t)/t]^2$.

With this established, we can now describe the time evolution of the isolated nodes, namely $N_1(t)$. At the next discrete time step, the number of isolated nodes is initially incremented by one with the addition of a new node. Yet, when a link is added (which happens with probability δ), the number of isolated nodes is decremented by one if the first chosen node is isolated or if either the second or third node is isolated. It is decremented by two if both the first node and either the second or third node is isolated. Therefore, the average number of components of size one can be obtained as

$$\begin{aligned} N_1(t+1) &= N_1(t) + 1 - \delta N_1(t)/t - \delta[s_1(t)^2 - s_2(t)^2] \\ &= N_1(t) + 1 - \delta N_1(t)/t - 2\delta N_1(t)/t + \delta[N_1(t)/t]^2. \end{aligned} \quad (2)$$

For larger components (i.e., $k > 1$), when an edge is added N_k decreases if the first node is in a component of size k . It also decreases if the smaller of the second and third components considered are of size k . In contrast, N_k increases when two smaller components, one of size $k - j$ and one of size j , merge to form a component of size k . Therefore,

$$\begin{aligned} N_k(t+1) &= N_k(t) - \delta N_k(t)/t - \delta[s_k(t)^2 - s_{k+1}(t)^2] \\ &\quad + \delta \sum_{j=1}^{k-1} jN_j(t)[s_{k-j}(t)^2 - s_{k-j+1}(t)^2]/t \\ &= N_k(t) - \delta N_k(t)/t - \delta 2kN_k(t)s_k(t)/t \\ &\quad + \delta k^2[N_k(t)/t]^2 \\ &\quad + \delta \sum_{j=1}^{k-1} jN_j(t)[s_{k-j}(t)^2 - s_{k-j+1}(t)^2]/t. \end{aligned} \quad (3)$$

Following Ref. [7], we now pose the ansatz that, in the limit $t \rightarrow \infty$, the average number of components of size k takes the form $N_k(t) = a_k t$, where a_k is a constant independent of time. We also define $s_k = \lim_{t \rightarrow \infty} s_k(t)$. The fraction of nodes that belong to components of size k is given by ka_k . Substituting these variables into Eqs. (2) and (3) and taking the limit provides, for $k = 1$,

$$a_1 = 1 - \delta(3a_1 - a_1^2), \quad 0 = \delta a_1^2 - (3\delta + 1)a_1 + 1. \quad (4)$$

Similarly, for $k > 1$, we obtain

$$a_k = -\delta(a_k + 2ks_ka_k - k^2a_k^2) + \delta \sum_{j=1}^{k-1} ja_j(s_{k-j}^2 - s_{k-j+1}^2).$$

Rearranging this equation, we arrive at the condition:

$$\begin{aligned} 0 &= \delta k^2 a_k^2 - [(1 + 2ks_k)\delta + 1]a_k \\ &\quad + \delta \sum_{j=1}^{k-1} ja_j(s_{k-j}^2 - s_{k-j+1}^2). \end{aligned} \quad (5)$$

Solving for a_1 , we obtain the two solutions $a_1 = \frac{1}{2\delta}(3\delta + 1 \pm \sqrt{9\delta^2 + 2\delta + 1})$. Since a_1 is the ratio of isolated nodes to the total number of nodes present in the network, we require that $a_1 \leq 1$ for all values of δ . Using the above

constraint, we eliminate one of the two solutions to get $a_1 = \frac{1}{2\delta}(3\delta - \sqrt{9\delta^2 + 2\delta + 1})$. We note that the equation for a_k only depends on a_j 's where $j < k$. Thus, having solved for a_1 we can recursively solve for each a_k with $k > 1$ starting with a_2 . From our simulations we find that $a_{k+1} < a_k$ for all values of δ . Using this as a condition, we are able to select a single solution for each a_k . We also note that, since we numerically solve for the a_k 's, we can only solve for a finite number of them. The maximum value of k solved for via numerical iteration of Eq. (5) is denoted k_m . For a given level of accuracy, we would need to use larger values of k_m the closer we are to the critical point. We also verify the ansatz that $N_k(t)/t$ goes to a constant a_k in the limit of $t \rightarrow \infty$ is indeed true for the AE-CHKNS process.

IV. RESULTS

A. Fractional size of the largest component

We denote the fractional size of the largest component by S . In other words, S is the ratio of the number of nodes in the largest component to the total number of nodes in the network. As the value of δ is increased, S increases from zero to a nonzero value; it is the order parameter for this phase transition. The fractional size of the largest component can be obtained from the a_k values as

$$S = 1 - \lim_{k_m \rightarrow \infty} \sum_{k=1}^{k_m} k a_k. \quad (6)$$

Figure 2 shows the fractional size of the largest component obtained from Monte Carlo simulations of the graph evolution process and from the values found for a_k using Eqs. (4) and (5). The critical point is the smallest value of δ for which S becomes nonzero in the asymptotic limit. From Fig. 2 we can see that the critical point (δ_c) for AE-CHKNS clearly lies in the region $0.3 < \delta_c < 0.4$.

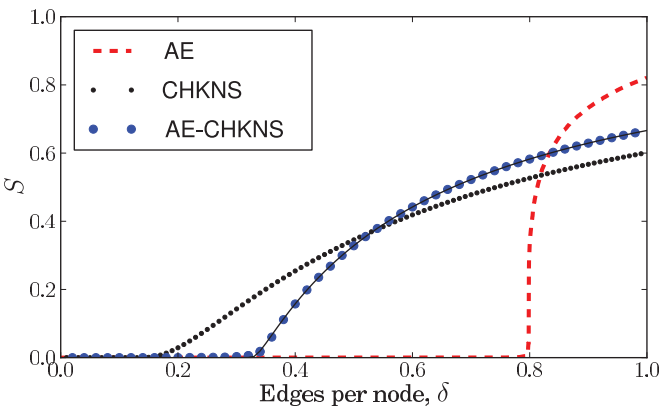


FIG. 2. (Color online) Fractional size of the largest component as a function of δ for the CHKNS model, AE percolation, and AE-CHKNS. Solid line: Analytic behavior predicted for AE-CHKNS via Eq. (6) evaluated by numerically solving Eq. (5) up to $k_m = 2 \times 10^4$. Circles are obtained from Monte Carlo simulations of the network with $N = 10^5$ nodes with each point averaged over 100 realizations. Error bars are smaller than the size of the marker. The results for AE percolation and CHKNS model are from Refs. [7] and [25], respectively.

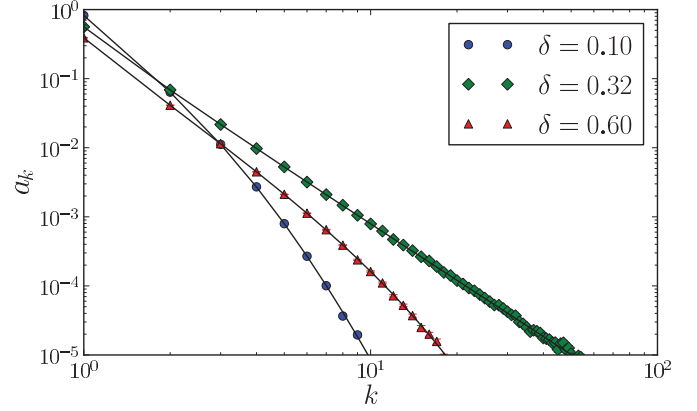


FIG. 3. (Color online) Plotted is a_k versus k , the fraction of nodes belonging to components of size k , for three different values of δ for the AE-CHKNS process. Solid lines: theoretical results obtained from solving Eqs. (4) and (5). Markers: simulation averaged over 10^5 realizations. The error bars are smaller than the size of the marker.

B. Average number of components of a given size

In the limit $t \rightarrow \infty$, the ka_k values, which can be obtained from Eqs. (4) and (5), correspond to the fraction of nodes in the network that belong to components of size k . Figure 3 shows the distribution of a_k for three different values of δ , including results from the direct Monte Carlo simulations (solid symbols) and from the numerical solution (solid lines) obtained by iteratively solving Eqs. (4) and (5). The excellent agreement between the simulations and the numerical solution indicates that our analytic equations successfully estimate the a_k values for different values of δ .

In Sec. IV A, we were able to deduce that the critical point lies in the region $0.3 < \delta_c < 0.4$. In the vicinity of the critical point (e.g., $\delta = 0.32$ on Fig. 3), a_k versus k exhibits a power-law. For smaller values of δ (e.g., $\delta = 0.10$ on Fig. 3) and for larger values (e.g., $\delta = 0.60$ on Fig. 3), a_k versus k falls faster than a power-law (i.e., exponentially). In the next section we take advantage of this behavior to refine our estimate of the critical point.

C. Estimating the critical point

Traditional methods of determining the critical point involve looking at the smallest value of δ where the fractional size of the largest component S is nonzero or the point where the susceptibility χ is nonanalytic. However, we were unable to obtain a closed form expression for S and χ . Although we can estimate these quantities with summations involving a_k [Eqs. (6) and (7)], we have to truncate these summations at a finite value of k (i.e., k_m). Such truncated S and χ prove to be ill-suited for estimating δ_c . This section presents an alternative method founded on the assumption that, like other physical quantities [38,39], a_k versus k exhibits a power-law behavior ($a_k \sim k^{-C}$) at the critical point. This alternate method proves much more appropriate for estimating δ_c in the presence of truncation.

Our observations reveal that, for $\delta \neq \delta_c$ but sufficiently close, a_k versus k shows an algebraic decay for small values of k followed by a sharper (exponential) decay when k is large. Therefore, we fit the a_k values to a power-law with

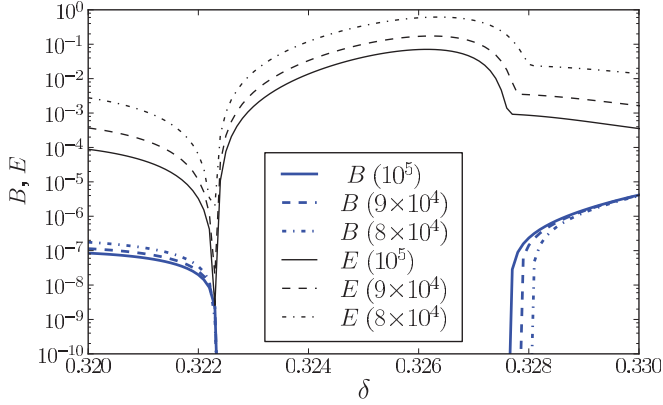


FIG. 4. (Color online) Fitting $a_k = Ak^{-C} \exp(-Bk)$ for different values of δ and k_m [the maximum value of k solved for in Eq. (5)]. Plotted are B values obtained from best fits and the associated error E , with k_m values indicated in parentheses. Both B and E show a sharp drop at $\delta = 0.3223$, indicating the distribution is an exact power-law in the vicinity of that point. While the point at which B goes to zero with increasing δ does not change with k_m , the point at which B again becomes nonzero shifts to the left as we increase the value of k_m , indicating that in the truly infinite limit the exponential cutoff parameter, B , will be zero only at the critical point.

an exponential decay [i.e., $a_k = Ak^{-C} \exp(-Bk)$] for various values of δ around the critical point. By our assumption that a_k should be exactly power-law distributed for $\delta = \delta_c$, we expect this fitting function to *exactly* reproduce the data with the parameter $B = 0$ at the critical point. The goodness of fit is estimated by using the sum of squares of the difference between the fit and a_k values, which we refer to as the error (E). Figure 4 shows how both the error and the value of the parameter B , which controls the onset of exponential decay, drop by several orders of magnitude at $\delta = 0.3223$. (Note, if $B \rightarrow 0$, we recover a pure power law, $a_k = Ak^{-C}$.)

The parameter B and the error E are shown for three different values of k_m in Fig. 4. (Recall k_m is the maximum value of k up to which we solve for a_k 's.) We note that as δ increases, the B values for the three different values of k_m drop at $\delta = 0.3223$, but the point where B starts to increase again differs for different values of k_m . From Fig. 4 we can see that this point, where B starts to increase again, has the value $\delta \approx 0.328$ for the smallest k_m shown and that it decreases with increasing k_m . This suggests that as $k_m \rightarrow \infty$, the point where B becomes nonzero moves leftward and ultimately coincides with the point where B becomes zero, i.e., B is zero at exactly one point ($\delta \approx 0.3223$). From Fig. 4 we can see that the distribution of the a_k 's follows a power-law in the vicinity of $\delta_c \approx 0.3223$ with an accuracy of $\pm 2 \times 10^{-4}$. At $\delta = \delta_c$, the fitting routine gives the best fit value of the exponent $C \approx 2.68$. For $\delta > \delta_c$, the errors E grow rapidly because the a_k values no longer fit a power-law with an exponential decay.

D. Susceptibility

The susceptibility χ is defined to be the average size of the component to which a randomly chosen node belongs (excluding the giant component, if any). It can be expressed in

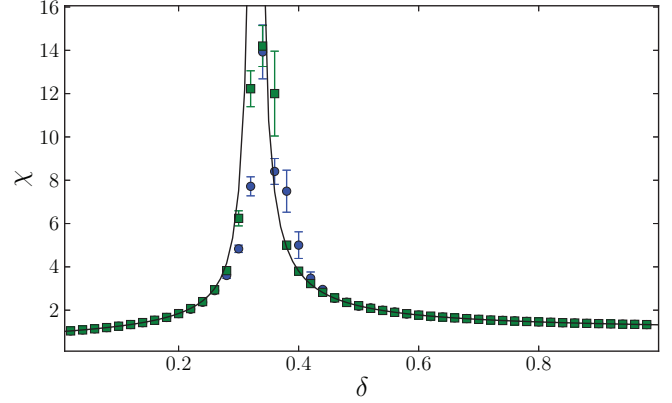


FIG. 5. (Color online) Susceptibility χ (average size of a component to which a randomly chosen node belongs) as a function of edge density, δ . Markers: numerical simulations averaged over 100 realizations for system sizes $N = 10^4$ (circles) and $N = 10^5$ (squares). Solid lines: analytical results obtained by truncating the sums of Eq. (7) at $k_m = 2 \times 10^4$.

terms of a_k 's as

$$\chi = \lim_{k_m \rightarrow \infty} \frac{\sum_{k=1}^{k_m} k^2 a_k}{\sum_{k=1}^{k_m} k a_k}. \quad (7)$$

Figure 5 shows, for both theory and simulations, how χ varies as a function of δ . Note that if a_k decays as a power law with exponent γ , then the numerator of Eq. (7) (and thus χ) diverges when $\gamma < 3$. Recall from Sec. IV C that at the critical point $a_k \sim k^{-C}$ with $C \approx 2.68$. This implies that, for AE-CHKNS, χ diverges at the critical point, as corroborated in Fig. 5. In contrast, the susceptibility in the CHKNS model exhibits a discrete jump at the critical point but remains finite. Note that in the CHKNS model, for $\delta = \delta_c$, $a_k \sim 2k^{-3}(\log k)^{-1}$ [18], which results in a χ that converges to a finite value for all values of δ . The divergence in the average component size indicates a broader component distribution for AE-CHKNS when compared to the CHKNS model.

E. Critical scaling: Infinite-order phase transition

The nature of a phase transition is characterized by the way the order parameter behaves close to the critical point. This behavior governs how the system evolves from one phase to another and has significant bearing on the dynamics of the system close to the critical point. Traditionally studied percolation transitions, such as the one exhibited by the Erdős-Rényi model, are second order. For a second-order phase transition, the parameter S scales as

$$S \sim (\delta - \delta_c)^\gamma, \quad (8)$$

for $\delta > \delta_c$ [38]. There also exist systems where the transition has a much smoother behavior as observed in models such as the CHKNS model. These transitions can typically be characterized by the following scaling relationship

$$S \sim e^{\alpha(\delta - \delta_c)^{-\beta}}, \quad (9)$$

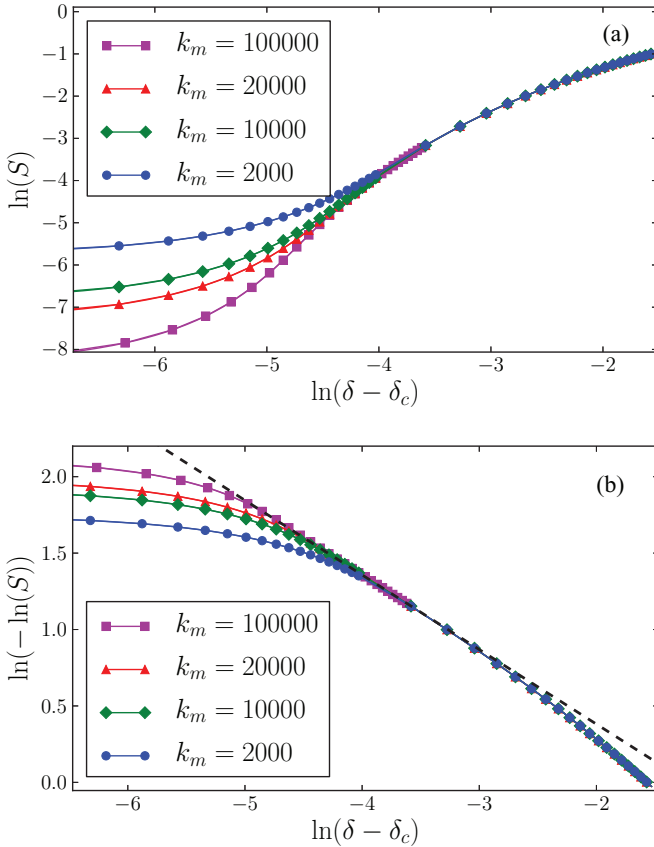


FIG. 6. (Color online) The fractional size S of the largest component close to the critical point. Eq. (6) was evaluated numerically to obtain S for different values of k_m in order to show the effect of truncation. (a) The absence of a linear segment in the plot of $\ln S$ vs. $\ln(\delta - \delta_c)$ indicates that this phase transition is not second order. (b) The presence of a linear segment, best fit by the dashed line in the plot of $\ln(-\ln S)$ vs. $\ln(\delta - \delta_c)$ is indicative of an infinite-order phase transition.

for $\delta > \delta_c$. Since the order parameter has an exponential form, it is infinitely differentiable and the resulting phase transition is known to have infinite order.

Figure 6 shows the plot of S , the fractional size of the largest component, as a function of $\delta - \delta_c$ in two different scales. Figure 6(a) is a plot with both axes on a log scale for different choices of the maximum values of k_m (the maximum k for which the a_k 's are computed). If S were to scale as $(\delta - \delta_c)^\nu$ close to the critical point, we should see a straight line on the left-hand side of the plot. The absence of a linear segment shows that the phase transition is not of second order. We also verify that slightly changing the value of δ_c does not give us a straight line on this plot. Figure 6(b) shows $\ln(-\ln S)$ as function $\ln(\delta - \delta_c)$ for different choices of k_m . For an infinite-order process, in the limit $k_m \rightarrow \infty$ we should see a straight line for small positive values of $\delta - \delta_c$ (left-hand side of the plot). In contrast to Fig. 6(a), in Fig. 6(b) there is a linear segment, the length of which increases as we increase the value of k_m . This indicates that the transition is of infinite order [see Eq. (9)]. Using $k_m = 5 \times 10^5$, we estimate the slope of this segment to be -0.50 ± 0.01 , which indicates that, similar to the CHKNS model, the AE-CHKNS model also

exhibits scaling behavior with $\beta = 0.50 \pm 0.01$. With respect to the second scaling parameter, for AE-CHKNS we find that $\alpha = -0.53 \pm 0.03$, which is higher than the value found for the CHKNS model where $\alpha = -\pi/\sqrt{8} \simeq -1.1107$ [19,40]. This implies that although both AE-CHKNS and CHKNS share the same functional form for the growth of the fractional size of the largest component, AE-CHKNS has a faster rate.

V. DISCUSSION AND CONCLUSION

In this manuscript we introduce and study (both analytically and numerically) a model of a growing network with competition between edges. Starting from a small collection of seed nodes, at each discrete time step a new node arrives and with probability δ a new edge is added through a competitive process according to the adjacent edge rule. Without edge competition (i.e., the original CHKNS model), the critical point is $\delta_c = 1/8$. For our model (i.e., the AE-CHKNS model), $\delta_c \simeq 0.3223$. Thus, the ability to choose between two random edges can delay the emergence of large-scale connectivity by a factor of more than two. We also provide strong evidence that, despite the addition of edge-choice to the model, the phase transition remains infinite order rather than becoming second order. There is a difference, however, in the behavior of the susceptibility. The susceptibility diverges at the critical point in the AE-CHKNS model while it remains bounded in the CHKNS model.

Delaying percolation through a competitive edge process has been the focus of many studies in recent years, and these studies indicate that delaying percolation leads to an abrupt, “explosive” transition [20–25,37,41–45]. (The transition appears discontinuous on any finite system and in the thermodynamic limit has a universality class distinct from standard second-order transitions.) Here we show that node arrival can temper this effect of edge competition. The interplay of node and edge arrival in the AE-CHKNS model allows us to considerably delay the percolation transition but achieve an infinitely smooth transition. This opens possibilities for network design and control. For instance, a smooth transition allows for the detection of large-scale connectivity while it is still quite limited, allowing time to enact network interventions. Thus, with node arrival, one might effectively achieve the twofold goal of delaying large-scale connectivity while enhancing opportunities for network interventions.

We should note the extremely different initial conditions of the CHKNS and the AE models. CHKNS is initialized with a small set of seed nodes, $N_0 = O(1)$. In contrast, AE is initialized with a large collection of seed nodes, N_0 , and analyzed in the limit $N_0 \rightarrow \infty$. The AE-CHKNS model introduced here uses the initial conditions of CHKNS. Another important fact to note is that in the AE-CHKNS model, since δ is defined as the probability of adding an edge, the rate of edge arrival can never exceed the rate of node arrival. We also note that many real-world networks, from online social networks to electric power grids, have edge density that increases over time [46–48].

Future work could explore different regimes between the AE-CHKNS and the AE model, especially if edges arrive more frequently than nodes. Starting with N_0 nodes and no edges at time $t = N_0$, a process similar to the following could be

used to grow a graph of N nodes with edge density δ . At each discrete time step:

- (1) A node is added to the graph.
- (2) A number is drawn from a Poisson distribution of mean $\delta/(1 - N_0/N)$. That many edges are added to the graph according to the AE rule.
- (3) If $t < N$, set $t \rightarrow t + 1$ and return to step 1.

In the limit $N \rightarrow \infty$, different regimes could be studied depending on how N_0 depends on N . There are two extremes. Using $N_0 = O(1)$ should result in a process very similar to AE-CHKNS with a smooth transition. On the other hand, using $N_0 = N - O(1)$ should result in an explosive transition similar to the AE percolation. We leave it to future work to explore the intermediate regimes, which may elucidate how much node arrival is necessary to mitigate the abrupt nature of the delayed phase transition.

Finally, it would also be interesting future work to investigate if growth is necessary to significantly delay the transition while preserving its smoothness, or if the intricate correlations introduced by the time ordering of the nodes could be reproduced through different means.

ACKNOWLEDGMENTS

We thank Steven Strogatz for suggesting the idea of combining growth and choice. This work was supported in part by the Defense Threat Reduction Agency Basic Research Award HDTRA1-10-1-0088, the Army Research Laboratory Cooperative Agreement No. W911NF-09-2-0053, NSF Grant No. ICES-1216048, and Fonds de recherche du Québec-Nature et technologies (Postdoctoral Fellowship Program).

-
- [1] R. Albert and A.-L. Barabási, *Rev. Mod. Phys.* **74**, 47 (2002).
 - [2] M. Newman, *Networks: An Introduction* (Oxford University Press, Oxford, 2010).
 - [3] P. Holme and J. Saramäki, *Phys. Rep.* **519**, 97 (2012).
 - [4] J. Leskovec, D. Chakrabarti, J. Kleinberg, C. Faloutsos, and Z. Ghahramani, *J. Mach. Learn. Res.* **11**, 985 (2010).
 - [5] V. Nicosia, G. Bianconi, V. Latora, and M. Barthelemy, *Phys. Rev. Lett.* **111**, 058701 (2013).
 - [6] A. Barabási and R. Albert, *Science* **286**, 509 (1999).
 - [7] D. S. Callaway, J. E. Hopcroft, J. M. Kleinberg, M. E. J. Newman, and S. H. Strogatz, *Phys. Rev. E* **64**, 041902 (2001).
 - [8] P. L. Krapivsky, S. Redner, and F. Leyvraz, *Phys. Rev. Lett.* **85**, 4629 (2000).
 - [9] A. Vázquez, *Phys. Rev. E* **67**, 056104 (2003).
 - [10] R. M. D'Souza and S. Roy, *Phys. Rev. E* **78**, 045101(R) (2008).
 - [11] B. Karrer and M. E. J. Newman, *Phys. Rev. Lett.* **102**, 128701 (2009).
 - [12] D. Stauffer and A. Aharony, *Introduction to Percolation Theory* (CRC Press, LLC, Boca Raton, 1994).
 - [13] M. Sahimi, *Applications of Percolation Theory* (CRC Press, LLC, Boca Raton, 1994).
 - [14] S. N. Dorogovtsev, A. V. Goltsev, and J. F. F. Mendes, *Rev. Mod. Phys.* **80**, 1275 (2008).
 - [15] P. Erdős and A. Rényi, *Math. Inst. Hung. Acad. Sci. Publ.* **5**, 17 (1960).
 - [16] R. Kumar, P. Raghavan, S. Rajagopalan, D. Sivakumar, A. Tomkins, and E. Upfal, in *Foundations of Computer Science, 2000. Proceedings of the 41st Annual Symposium on, Redondo Beach, CA* (IEEE, Piscataway, NJ, 2000), pp. 57–65.
 - [17] A. Vázquez, A. Flammini, A. Maritan, and A. Vespignani, *Complexus* **1**, 38 (2003).
 - [18] R. Durrett, *Random Graph Dynamics* (Cambridge University Press, Cambridge, 2006).
 - [19] B. Bollobás, S. Janson, and O. Riordan, *Random Struct. Alg.* **26**, 1 (2005).
 - [20] D. Achlioptas, R. M. D'Souza, and J. Spencer, *Science* **323**, 1453 (2009).
 - [21] R. A. da Costa, S. N. Dorogovtsev, A. V. Goltsev, and J. F. F. Mendes, *Phys. Rev. Lett.* **105**, 255701 (2010).
 - [22] P. Grassberger, C. Christensen, G. Bizhani, S. W. Son, and M. Paczuski, *Phys. Rev. Lett.* **106**, 225701 (2011).
 - [23] J. Nagler, A. Levina, and M. Timme, *Nat. Phys.* **7**, 265 (2011).
 - [24] S. Manna and A. Chatterjee, *Physica A* **390**, 177 (2011).
 - [25] R. M. D'Souza and M. Mitzenmacher, *Phys. Rev. Lett.* **104**, 195702 (2010).
 - [26] M. E. J. Newman, S. Forrest, and J. Balthrop, *Phys. Rev. E* **66**, 035101 (2002).
 - [27] M. Boguñá and R. Pastor-Satorras, *Phys. Rev. E* **66**, 047104 (2002).
 - [28] M. O. Jackson and B. W. Rogers, *Am. Econ. Rev.* **97**, 890 (2007).
 - [29] J. Kim, P. L. Krapivsky, B. Kahng, and S. Redner, *Phys. Rev. E* **66**, 055101 (2002).
 - [30] M. Middendorf, E. Ziv, and C. H. Wiggins, *Proc. Natl. Acad. Sci. USA* **102**, 3192 (2005).
 - [31] Note that the description of AE percolation in the original article is slightly different but equivalent. The original model is recovered if we set $\delta = 1$ and replace the stopping condition with $t = t_{\text{stop}}$. The control parameter thus becomes t_{stop}/N .
 - [32] H. K. Lee, B. J. Kim, and H. Park, *Phys. Rev. E* **84**, 020101 (2011).
 - [33] L. Tian and D.-N. Shi, *Phys. Lett. A* **376**, 286 (2012).
 - [34] O. Riordan and L. Warnke, *Science* **333**, 322 (2011).
 - [35] D. J. Aldous, *Bernoulli* **5**, 3 (1999).
 - [36] E. Ben-Naim and P. L. Krapivsky, *Phys. Rev. E* **71**, 026129 (2005).
 - [37] Y. S. Cho, B. Kahng, and D. Kim, *Phys. Rev. E* **81**, 030103 (2010).
 - [38] R. K. Pathria and P. D. Beale, *Statistical Mechanics*, 3rd ed. (Academic Press, Boston, 2011).
 - [39] M. Le Bellac, F. Mortessagne, and G. Batrouni, *Equilibrium and Nonequilibrium Statistical Thermodynamics* (Cambridge University Press, Cambridge, 2004).
 - [40] S. N. Dorogovtsev, J. F. F. Mendes, and A. N. Samukhin, *Phys. Rev. E* **64**, 066110 (2001).
 - [41] R. M. Ziff, *Phys. Rev. Lett.* **103**, 045701 (2009).
 - [42] F. Radicchi and S. Fortunato, *Phys. Rev. Lett.* **103**, 168701 (2009).

- [43] E. J. Friedman and A. S. Landsberg, *Phys. Rev. Lett.* **103**, 255701 (2009).
- [44] Y. S. Cho and B. Kahng, *Phys. Rev. Lett.* **107**, 275703 (2011).
- [45] K. Panagiotou, R. Spöhel, A. Steger, and H. Thomas, *Electr. Notes Discrete Math.* **38**, 699 (2011).
- [46] J. Leskovec, J. Kleinberg, and C. Faloutsos, *ACM Trans. Knowledge Disc. Data (TKDD)* **1**, 2 (2007).
- [47] M. Amin and J. Stringer, *Mat. Res. Soc. Bull.* **33**, 399 (2008).
- [48] S. Cass, *MIT Technol. Rev.* **114**, 70 (2011).